# CONSIDERATIONS IN THE USE OF QCMs FOR ACCURATE CONTAMINATION MEASUREMENT D. A. WALLACE

# BERKELEY CONTROLS INC. - IRVINE, CALIFORNIA

#### 1.0 INTRODUCTION

Piezoelectric quartz, flat plate crystals have been used as microbalances for the measurement of mass flux in free molecule flow since Sauerbrey's initial work in 1959 defined the nature of the crystal's frequency response to mass addition. The QCM, as this type of microbalance has come to be known, serves as the workhorse thickness monitor for thin film deposition processes as well as a tool for outgassing studies and, diagnostically, for molecular flux contaminant source identification on spacecraft.

In many applications of the QCM to date, qualitative measurements have been sufficient. However, in more analytical work such as that of Hughes, Allen, Linford and Bonham<sup>2</sup> or Glassford<sup>3,4</sup> or Liu and Glassford<sup>5</sup>, an accurate determination of molecular flux is essential for confirmation of theoretical models.

- Sauerbrey, G., 'Verwendung von Schwingquartzen zur Wagung dunner Schicten und vur Mikro Wagung'', Zeit, fur Physik, Vol. 155: 206-222 (1959).
- Hughes, T.A., Allen, T.H., Linford, R.M.F., and Bonham, T.E., <u>Investigation of Contamination Effects on Thermal Control Materials</u>, AFML-TR-74-218 (1975) Final Technical Report, Contract F33615-73-C-5091, McDonnell Douglas Corp.
- Glassford, A.P.M., An analysis of the accuracy of a commercial quartz crystal microbalance. AIAA Paper No. 76-438, presented at AIAA lith Thermophysics Conference, San Diego, Calif. (1976).
- Glassford, A.P.M., The response of a quartz crystal microbalance to a liquid deposit. Paper presented at the Space Simulation Conference, Los Angeles, California (1977).
- Liu, C.K., and Glassford, A.P.M., Kinetics data for diffusion of outgas species from RTV 560. Paper presented at the Space Simulation Conference, Los Angeles, Calif. (1977).

This paper will examine the flow equations involved in QCM molecular mass flux measurement, the effect of parameters such as crystal temperature, QCM entrance configuration and randomness of the flow and discuss the implications of these equations in measuring several materials' mass flux.

#### 2.0 TECHNICAL DISCUSSION

# 2.1 Basic Crystal Mass Flux

The crystal's sensitivity to mass deposition is proportional to the amplitude of surface displacement for a crystal in thickness shear vibration. The value, S, obtained by integration over the active area of the crystal is usually used as the crystal mass sensitivity factor, assuming uniform deposition on the crystal. Within the deposition range for which frequency shift is linearly related to mass deposition, i.e. approximately  $\Delta f < 0.01\ f_{_{\rm O}}$ , the mass flux equation for a crystal exposed on one side to a condensing gas is

$$\frac{\mathring{m}}{A} = S \frac{\Delta f}{\Delta t}$$
 (1)

Where S = crystal mass sensitivity, g/cm<sup>2</sup>-Hz
$$\mathring{m} = \text{mass flow, g/s}$$

$$A = \text{area, cm}^2$$

$$\Delta f = \text{frequency change, Hz}$$

$$\Delta t = \text{time interval, s}$$

If, rather than incoming flow, a deposited mass is evaporating from the crystal into an infinite sink, then,

$$\frac{\mathring{\mathbf{n}}}{\mathsf{A}}\bigg|_{\mathsf{evap}} = -\mathsf{S} \, \frac{\Delta \mathsf{f}}{\Delta \mathsf{t}} \tag{2}$$

It is important to realize that in most situations both types of flow are occurring and the crystal frequency change with time relates to both the incoming flow and the crystal temperature dependent evaporating flow as,

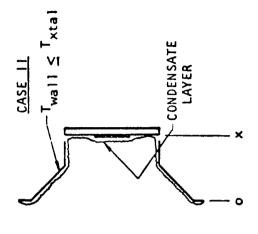
$$\frac{\mathring{\mathbf{n}}}{\mathbf{A}} = \mathbf{S} \left. \frac{\Delta \mathbf{f}}{\Delta \mathbf{t}} + \frac{\mathring{\mathbf{n}}}{\mathbf{A}} \right|_{\text{evap}} \tag{3}$$

# 2.2 Crystal Entrance Configuration

Obviously the determination of incoming mass flux using frequency change must include a consideration of the evaporating mass flux. The mass flux equation is further altered by the QCM entrance configuration. Figure 1, Case 1, shows a representative entrance section consisting of an entrance conical frustum (Station 0) and a cylindrical section leading to the crystal (Station X). The probability that an entering molecule will eventually reach the crystal and be captured is a function of the nature of the entering flux, i.e. diffuse or directed, the entrance configuration and the entrance wall temperature relative to the crystal temperature. If the flow is diffuse and the walls are warmer than the crystal (which is assumed to have unity sticking coefficient for the entering molecules) a conductance factor,  $K_{o-x}$ , can be determined. The evaporating molecules face a similar flow reduction in leaving the crystal since through wall collision some will return to the crystal, be recondensed and recycled back through the system. The evaporative flow conductance,  $K_{x=0}$ , is related through reciprocity to the entering flow conductance, Ko-x. The expression for this diffuse flow with warm entrance walls is,

$$\frac{\mathring{\mathbf{m}}}{\mathsf{A}}\Big|_{\mathsf{o}} = \frac{\mathsf{A}_{\mathsf{X}}}{\mathsf{A}_{\mathsf{o}}} \frac{\mathsf{S}}{\mathsf{K}_{\mathsf{o}-\mathsf{X}}} \frac{\Delta \mathsf{f}}{\Delta \mathsf{t}} + \frac{\mathring{\mathbf{m}}}{\mathsf{A}}\Big|_{\mathsf{evap}} \tag{4}$$

If the entrance walls are at the same or lower temperature as the crystal, Figure 1 Case II, the walls condense entering molecules which strike them and thus the entering and exiting flow conductance is altered from the previous warm wall case. The probability of a molecule passing directly through the frustrum without striking the



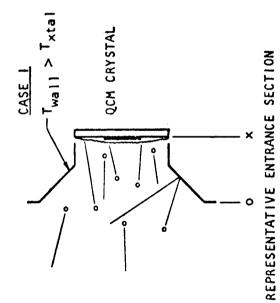


FIGURE 1 MASS FLUX MEASUREMENT WITH QCM ENTRANCE SECTION

wall and the further probability of the molecule reaching the crystal without collision, must be calculated i.e.  $K_{O-X}|_{direct}$ . An added element is added to the crystal mass flux by the evaporation of material from the walls which has a probability of striking the crystal before exiting the system,  $K_{W-X}|_{direct}$ . The expression for Case II is,

$$\frac{\mathring{\underline{m}}}{|A|}_{O} = \frac{S \frac{A_{x}}{A_{O}} \frac{\Lambda f}{\Delta t} + \frac{\mathring{\underline{m}}}{|A|} \frac{A_{x}}{|A|} \frac{A_{x}}{|A|} - \frac{A_{w}}{|A|} K_{w-x} |A| + \frac{\mathring{\underline{m}}}{|A|} + \frac{\mathring{\underline{m}}}{|A|} + \frac{\mathring{\underline{m}}}{|A|} + \frac{\mathring{\underline{m}}}{|$$

For this case with evaporation only,

$$\frac{\frac{\mathring{\mathbf{n}}}{A}\Big|_{e} = -\frac{\frac{S \frac{\Delta f}{\Delta t}}{1 - \frac{A_{w}}{A_{x}} K_{w-x}\Big|_{direct}}$$
(6)

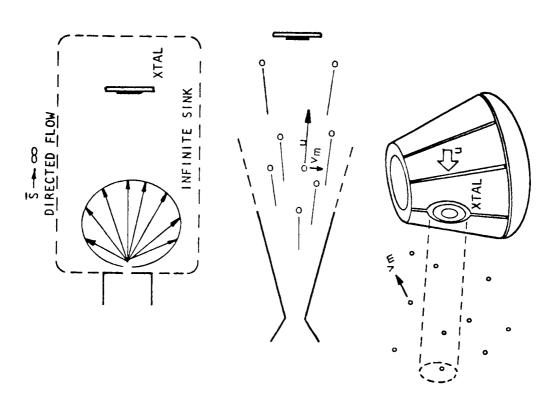
#### 2.3 Nature of Flow

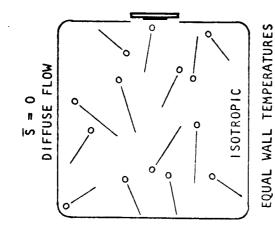
Free molecule flow is often thought of as wholly diffuse i.e. Maxwellian, in nature with the further assumption of the existence of an isotropic pressure, whereas in many cases a much altered velocity distribution exists. This is especially true in cryopumped chambers, nozzle flows and spacecraft situations. The degree of directionality in a flow field is characterized by the speed ratio,  $\bar{\mathbf{S}}$ , defined as the ratio of the directed velocity,  $\mathbf{u}$ , to the gas mean thermal velocity,  $\mathbf{v}_{\mathbf{m}}$ ,

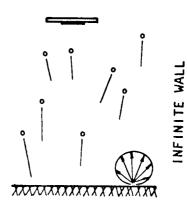
$$\bar{S} = \frac{u}{v_{m}} = \sqrt{\frac{2kT}{m}}$$
Where T = gas temperature
$$k = Boltzmann constant$$

$$m = molecule mass$$
(7)

Several illustrative examples of random and directed flow are given in Figure 2. Random, diffuse flow conditions exist in the enclosure shown with walls at equal temperature. A crystal facing an infinite outgassing wall sees molecules emanating from the wall according to







the cosine law which, in the aggregate, results in diffuse flow at the crystal.

On the other hand, the Knudsen cell shown in the figure with cosine distribution emanation of molecules, results in highly directional flow at the crystal since the enclosure is assumed to be an infinite sink. Only molecules from the aperature of the cell within the solid angle intersecting the crystal arrive at the crystal. There is no chance of collisions producing randomness. To a lesser extent, the same is true of nozzle flow. The nozzle imparts a mass motion, u, on the gas yet to a degree it still acts as a gas at rest with thermal velocity,  $v_{\rm m}$ . The spacecraft moving at high velocity, u, through the rarefied gas at rest with thermal velocity,  $v_{\rm m}$ , essentially sees molecules with a very high speed ratio striking the vehicle.

If we treat the limiting case of directed flow, i.e. collimated flow,  $\tilde{S}=\infty$ , shown in Figure 3, only the approaching flow within the envelope  $A_X$  can reach the crystal if the walls are considered to be condensing. Evaporation from the crystal and from the walls continues to be diffuse resulting in the expression for collimated mass flow to a cold wall QCM of,

$$\frac{\mathring{\mathbf{m}}}{\mathbf{A}}\Big|_{\mathbf{O}} = \mathbf{S} \frac{\Delta \mathbf{f}}{\Delta \mathbf{t}} + \frac{\mathring{\mathbf{m}}}{\mathbf{A}} \Big|_{\mathbf{evap}} \left[ 1 - \frac{\mathbf{A}_{\mathbf{W}}}{\mathbf{A}_{\mathbf{X}}} | \mathbf{K}_{\mathbf{W}-\mathbf{X}} \Big|_{\mathbf{direct}} \right]$$
(8)

Since evaporation is by nature diffuse it is independent of the nature of the entering flow. Thus equation (6) continues to apply for the case of evaporation only.

# 2.4 Measurement implications of Combined Flows

From the above equations it is evident that if an accurate determination of mass flux arriving at a QCM is to be deduced from crystal frequency shift information, the crystal temperature and to a certain extent the vapor pressure characteristics of the deposited material need to be known. An illustration of QCM response to

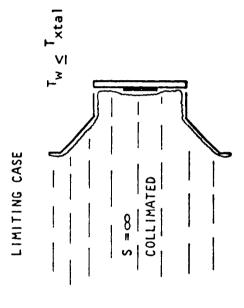


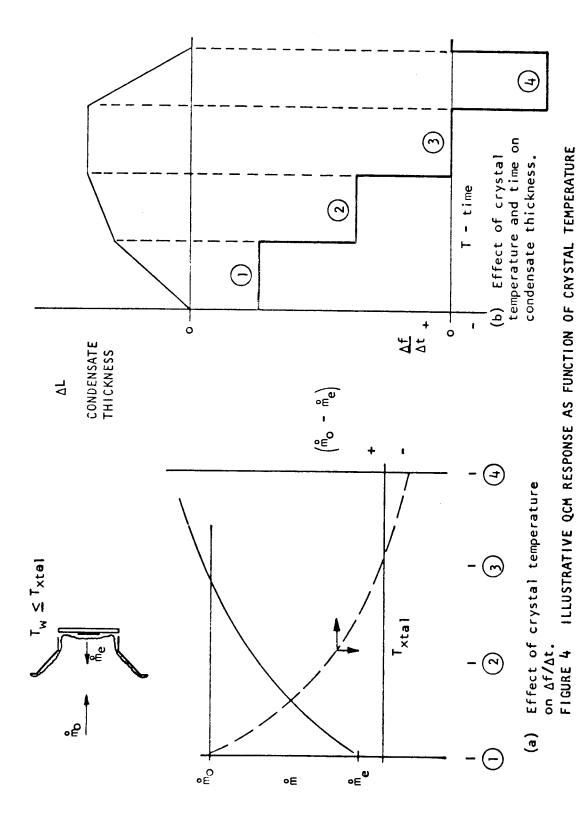
FIGURE 3 MASS FLUX MEASUREMENT WITH DIRECTED FLOW

crystal temperature change is shown in Figure 4(a). A case is shown for a cold wall QCM with constant entering mass flux,  $m_0$ , and changing evaporative mass flux,  $\mathring{m}_e$ , as a function of crystal temperature. For the low crystal temperature, 1,  $\mathring{m}_e$  is low,  $(\mathring{m}_0 - \mathring{m}_e)$  equals approximately  $\mathring{m}_0$  and the flow equations may be simplified accordingly. As the crystal temperature is increased to 2,  $(\mathring{m}_0 - \mathring{m}_e)$  decreases and thus  $\frac{\Delta f}{\Delta t}$  decreases until at 3  $\mathring{m}_e$  equals  $\mathring{m}_0$  and  $\frac{\Delta f}{\Delta t}$  is zero. If the crystal temperature is increased beyond this point, the evaporative flux exceeds the entering flux and a negative  $\frac{\Delta f}{\Delta t}$  is indicated.

The situation is further illustrated in Figure 4(b) where  $\mathring{\text{m}}_{\text{O}}$  is still assumed to be constant and the crystal temperature is held constant for some time interval. The initial low crystal temperature, 1, results in low evaporation and rapid condensate buildup with reduced growth rate for temperature 2 and no growth during the time the crystal is at temperature 3. The temperature 4 period reduces the condensate until all material is removed at which point of course the frequency change rate returns to zero. Without knowledge of either this entire cycle or the crystal temperature, it would be difficult in this case to distinguish between an absolutely clean QCM with  $\mathring{\text{m}}_{\text{O}}$  equal zero and a situation with a thick condensate and large entering and evaporating mass fluxes of equal magnitude. Both cases would produce zero frequency shift.

#### 2.5 Vapor Pressure Characteristics

The importance of the earlier statements concerning combined flow of incoming and evaporating flows on QCMs becomes evident as we consider the measurement of flows of specific gases. Figure 5 shows the vapor pressure characteristics of water vapor, a family of polydimethylsiloxanes and DC 704 silicone oil vapor. Water vapor is a major outgassing component in most vacuum systems and as such may be the primary constituent of the system background pressure. If it is desirable to measure the water vapor flux in a chamber at



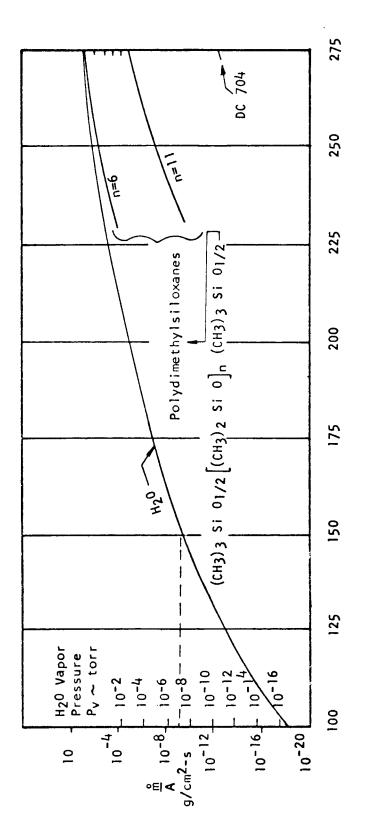


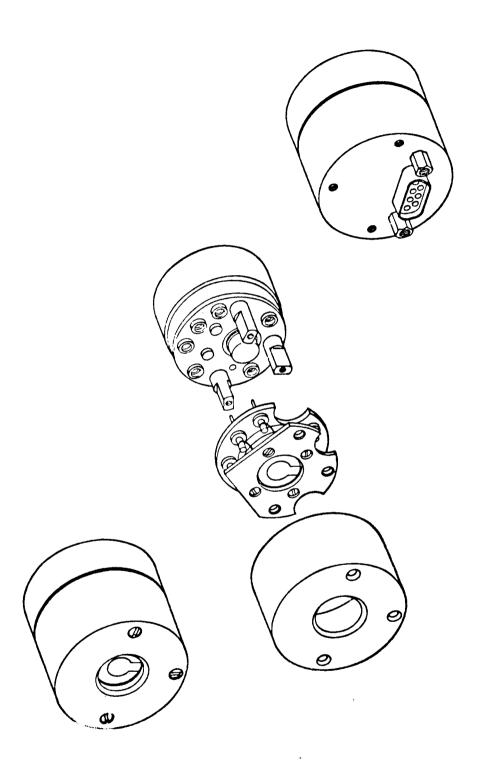
FIGURE 5 VAPOR PRESSURE, EVAPORATION RATE CHARACTERISTICS

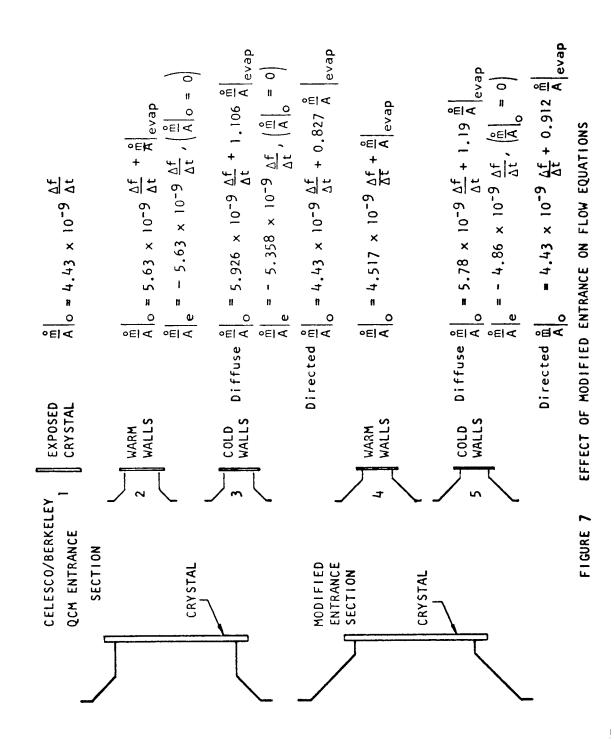
10<sup>-7</sup> torr for instance, the graph indicates QCM temperatures below 150°K must be used. At crystal temperatures above this level, evaporation would simply prevent the condensate formation on the crystal. This, of course, can be a definite advantage in situations where outgassing rates of materials such as various RTVs are to be measured without the complication of water vapor condensation. From the graph it is obvious that a crystal temperature of for instance -50°C, would collect the higher moleculer weight polydimethylsiloxanes with low reevaporation rates, whereas water vapor in the system would be at vapor pressures above  $10^{-2}$  torr and would not be sensed by the QCM. The observation may be made that indeed at this temperature the QCM would not respond to any but a major ambient air leak in the immediate vicinity of the QCM. DC 704 oil vapor on the other hand is collected by the QCM readily at temperatures near ambient. Measurement of the flow of other atmospheric gases such as nitrogen, oxygen and argon by the QCM require crystal temperatures below  $20^{\rm o}{\rm K}$ to achieve acceptably low reevaporation rates while hydrogen's vapor pressure is still in the 10<sup>-7</sup> torr range at 4.2°K.

Determination of the proper QCM sensing crystal temperature must consider then both the levels of incoming flux and evaporation rates, if accurate flux measurements are to be made.

## 2.6 Equations applied to an example QCM

To illustrate the magnitude of the effects discussed earlier, consider the Celesco/Berkeley cryogenic QCM sensor shown in Figure 6. The sensing crystal is mounted in a stress-free ring mount which allows the sensor to operate to below 20°K. The crystal temperature is sensed by a platinum resistance element located immediately behind the crystal. The performance accuracy of this sensor has been studied by Glassford<sup>3</sup>. Of interest to this discussion is the entrance section to the crystal which is shown in greater detail in Figure 7(a). The flow equations for this sensor with both warm and cold walls and





diffuse and directed flows, are shown in this Figure in comparison to an ideal exposed 10 MHz crystal. The entrance section which intuitively would seem to expose the crystal quite openly, is seen in fact to alter the mass sensitivity by 21% in the case of warm walls and by 25% for cold walls which do exist on this sensor. Modifying the entrance section as shown in Figure 7(b) significantly increases the flow conductance, as indicated by the reduced values in the equations. The important point here is not the relative merits of one entrance section over another, but simply that the flow conductance must be correctly known and used in the flow equation rather than an assumed exposed crystal sensitivity value if accurate flow measurements are to be made with the QCM.